Proc. Nat. Acad. Sci. USA
Vol. 73, No. 2, pp. 486–490, February 1976
Biophysics

Application of polarization effects in light scattering: A new biophysical tool

(bacterial spores/cell structure/nondestructive probe)

W. S. BICKEL, J. F. DAVIDSON, D. R. HUFFMAN, AND R. KILKSON

Department of Physics, University of Arizona, Tucson, Ariz. 85721

Communicated by Willis E. Lamb, Jr., November 20, 1975

ABSTRACT **We demonstrate that a newly developed instrument which measures all polarization and intensity information contained in differentially and elastically scattered light has valuable applications in biology. The polarization states of light scattered differentially from suspensions of biological scatterers are shown to contain structural information about those systems. The scatterers are discussed in the context of a 16 component matrix which completely characterizes the scattering process. The instrument and method are described in terms of the corresponding matrix algebra. We also discuss the use of the instrument as a device for distinguishing between closely related structural systems and as a tool for following time-dependent structural changes.**

A technique has recently been developed (1) which can measure *all* possible information contained in the light differentially and elastically scattered from a suspension of small particles. We used the technique to examine the polarization states of light scattered from suspensions of bacterial spores and showed that it will have valuable and powerful applications in biology. Initial results show that of 10 possible scattering parameters, one in particular is extremely valuable as an indicator of structural changes in biological systems. This parameter can distinguish between two mutant varieties of bacterial spores more easily than the differential scattered light intensity does.

Light scattering is widely used in biological research to determine particle numbers, particle sizes, axial ratios, size distributions, particle mobilities, and indices of refraction. Most of these studies measure only the small-angle differential scattered light intensity even though much more additional information is contained in the polarization states of the differentially scattered light. Previous studies of polarization effects have been restricted mostly to optical rotatory dispersion (ORD) and circular dichroism (CD) measurements in the forward direction, which do not contain the available angular information. Current research, however, indicates that polarization measurements are extremely valuable as system probes. In experiments with bacteria, Wyatt and Phillips (2) have shown depolarization of the differential scattered light intensity relative to the incident light. In the ultraviolet range, λ 2000–3000 Å, there are strong ORD and CD effects. Maestre and Tinoco (3, 4) have shown that viruses have very characteristic ORD and CD signals, uniquely defined by their nucleic acid and protein packing, and that the signals are sensitive to even the slightest modifications in their molecular arrangement. Subsequent studies (5, 6) have shown that corrections to polarization effects from Mie scattering must be made to ORD and CD measurements. However, these experiments neglect the detailed angular distribution of polarization.

Abbreviations: ORD, optical rotatory dispersion; CD, circular dichroism.

Therefore, the measurement of the 10 scattering parameters (light intensity *and* all polarization states) as functions of angle and wavelength will provide additional significant information about biological scattering systems. Our results show that this is the case.

The Scattering Matrix. The formal theory of elastic light scattering deals with Maxwell's equations, boundary conditions, and idealized physical models for the scatterer, and matrix algebra, which manipulates the interaction matrices, and light vectors, which describe the optical system, ignoring the exact mechanism causing the scattering. The fundamental problem of deriving structural features of the scatterer from scattering information is presently unsolvable for most biophysical cases. However, the matrix algebra can be used to catalog the scattering signals, which are related to the matrix elements involved in the scattering process.

A detailed discussion of the general scattering matrix is given in van de Hulst (7). We will review the role of Rayleigh and Mie particles and their relationships to biological particles, and then give an example of the matrix multiplication implied by a particular arrangement of the optical components to show how matrix elements are measured. We will then discuss some matrix element signals we measured to show their significance to biological systems.

A scatterer changes the state of the incoming polarized light by mixing the initial polarization states of the incident electric field vectors E_{lo} and E_{ro}. E_{lo} and E_{ro} are the initial components parallel and perpendicular to the scattering plane, respectively. The new parallel and perpendicular electric field components E_l and E_r arise through an interaction represented by mixing coefficients A_i.

$$\begin{aligned} E_l &= A_2E_{lo} + A_3E_{ro} \\ E_r &= A_4E_{lo} + A_1E_{ro} \end{aligned} \quad \text{or} \quad \begin{vmatrix} E_l \\ E_r \end{vmatrix} = \begin{bmatrix} A_2 & A_3 \\ A_4 & A_1 \end{bmatrix} \begin{vmatrix} E_{lo} \\ E_{ro} \end{vmatrix}. \quad [1]$$

The Stokes vector $|V|$, which completely characterizes the intensity and polarization of a light ray, is defined in terms of time averages of the electric field components of an electromagnetic wave:

$$\begin{aligned} I &= \langle E_lE_l^* + E_rE_r^* \rangle \\ Q &= \langle E_lE_l^* - E_rE_r^* \rangle \\ U &= \langle E_lE_r^* + E_rE_l^* \rangle \\ V &= \langle i(E_lE_r^* - E_rE_l^*) \rangle \end{aligned} \quad \text{or} \quad \begin{vmatrix} I \\ Q \\ U \\ V \end{vmatrix}$$

$$= \begin{vmatrix} \langle E_lE_l^* + E_rE_r^* \rangle \\ \langle E_lE_l^* - E_rE_r^* \rangle \\ \langle E_lE_r^* + E_rE_l^* \rangle \\ \langle i(E_lE_r^* - E_rE_l^*) \rangle \end{vmatrix} = |V|. \quad [2]$$

Here I = total intensity, Q = polarization at 0° or 90° to the scattering plane, U = polarization at ±45° to the scattering plane, and V = left or right circular polarization. The transformation of an incident four-component Stokes vector $|V_o|$ by a scattering matrix $[S]$ gives a final Stokes vector $|V_f|$ where $|V_f| = [S]|V_o|$ or

$$\begin{vmatrix} I_f \\ Q_f \\ U_f \\ V_f \end{vmatrix} = \begin{bmatrix} S_{11} & S_{12} & S_{13} & S_{14} \\ S_{21} & S_{22} & S_{23} & S_{24} \\ S_{31} & S_{32} & S_{33} & S_{34} \\ S_{41} & S_{42} & S_{43} & S_{44} \end{bmatrix} \begin{vmatrix} I_o \\ Q_o \\ U_o \\ V_o \end{vmatrix}. \quad [3]$$

When the values of the Stokes vector [2] are inserted into the matrix representation [3] one gets the general form of the scattering matrix given by van de Hulst (7). Any component of the electric field vector E can be written explicitly in terms of its phase ϵ, amplitude a, wave number k, and frequency ω. We have $E = a \exp[-i\epsilon] \exp[-i(kz - \omega t)]$. This vector is used to get the matrix that gives a direct relationship between the amplitudes a_i ($i = j$ or k) and the phase difference $\delta = \epsilon_j - \epsilon_k$. Then $A_kA_k^* = |a_k|^2$; $(A_jA_k^* + A_kA_j^*) = |a_j||a_k|\sin\delta$; and $i/2(A_jA_k^* - A_kA_j^*) = |a_j||a_k|\cos\delta$; and we get:

which is well known for the differential scattered light intensity signal from polydispersed systems.

Biological Particles. Biological particles are generally complex arrangements of various shaped structures, often having large size distributions resulting in relatively little structure in the differential scattered light intensity S_{11}. However, complex structure does occur on other S_{ij} signals, as shown by our preliminary work with selected biological systems. The matrix elements we studied in this experiment are:

$$S_{11} = \tfrac{1}{2}(a_1^2 + a_2^2 + a_3^2 + a_4^2);$$

$$\frac{S_{12}}{S_{11}} = \frac{(-a_1^2 + a_2^2 - a_3^2 + a_4^2)}{(a_1^2 + a_2^2 + a_3^2 + a_4^2)};$$

$$\frac{S_{13} + S_{33}}{S_{11} + S_{31}} = \frac{(a_3a_2 - a_4a_1 + a_2a_1 + a_3a_4)\cos\delta}{\tfrac{1}{2}(a_1^2 + a_2^2 + a_3^2 + a_4^2) + (a_2a_4 + a_3a_1)\cos\delta};$$

$$S^*_{34} = \frac{S_{14} + S_{34}}{S_{11} + S_{13}} = \frac{(a_1a_2 + a_3a_4)\cos\delta - (a_2a_3 + a_4a_1)\sin\delta}{\tfrac{1}{2}(a_1^2 + a_2^2 + a_3^2 + a_4^2) + (a_2a_3 + a_4a_1)\cos\delta}.$$

$$[S] = \begin{bmatrix} \tfrac{1}{2}(a_1^2 + a_2^2 + a_3^2 + a_4^2) & \tfrac{1}{2}(-a_1^2 + a_2^2 - a_3^2 + a_4^2) & (a_3a_2 - a_4a_1)\cos\delta & -(a_2a_3 + a_4a_1)\sin\delta \\ \tfrac{1}{2}(-a_1^2 + a_2^2 + a_3^2 - a_4^2) & \tfrac{1}{2}(a_1^2 + a_2^2 - a_3^2 - a_4^2) & (a_3a_2 - a_4a_1)\cos\delta & -(a_2a_3 - a_4a_1)\sin\delta \\ (a_2a_4 + a_3a_1)\cos\delta & (a_2a_4 - a_3a_1)\cos\delta & (a_2a_1 + a_3a_4)\cos\delta & -(a_2a_1 - a_3a_4)\sin\delta \\ (a_2a_4 + a_3a_1)\sin\delta & (a_2a_4 - a_3a_1)\sin\delta & (a_2a_1 + a_3a_4)\sin\delta & (a_2a_1 + a_3a_4)\cos\delta \end{bmatrix}. \quad [4]$$

The general scattering matrix given above applies to *any* system of particles. However, it is convenient to divide the particles into two rather broad ranges depending on the ratio of wavelength λ to particle size d. The two classes of scattering particles are called Rayleigh and Mie particles.

Rayleigh Particles ($d \ll \lambda$). Particles smaller than the wavelength λ of the incident radiation are called "small particles" or Rayleigh particles. For this condition ($d \ll \lambda$) the scattering matrix can be *exactly* calculated. It has the form:

$$[S] = \text{constant} \begin{bmatrix} 1 + \cos^2\theta & \sin^2\theta & 0 & 0 \\ \sin^2\theta & 1 + \cos^2\theta & 0 & 0 \\ 0 & 0 & \cos\theta & 0 \\ 0 & 0 & 0 & \cos\theta \end{bmatrix}.$$

The differential scattered light intensity is contained in the S_{11} matrix element and depends on the size, optical constants, and number density of the scatterers. Small particles which have anisotropic optical constants may have additional non-zero–off-diagonal matrix elements (7, 8).

Mie Particles ($d \geq \lambda$). Particles larger than the wavelength of the incident radiation are called "large particles" or Mie particles. In this case, only a few particle configurations can be treated exactly by theory. They are spherical particles (9), the infinite cylinder (10), and the infinite slab (11). Some variations of spherical particles, the spherical shell (7) and spherical particle with optical activity, have been recently treated theoretically (12, 13).

In general, signals from uniform sized and shaped (monodispersed) Mie particles are highly structured, the phase of the structure depending on the particle size, shape, and index of refraction. Therefore, small variations from monodisperseness can wash out the structure completely, an effect

Theoretically the S^*_{34} matrix combination is unique in comparison to other matrix elements. The presence of the phase terms $\cos\delta$ and $\sin\delta$ can cause a sign change in S^*_{34} for very small changes of δ. The larger number of possibilities for zeros and oscillations about zero contribute to the larger structure on the S^*_{34} signal as compared to the other matrix elements and matrix element combinations listed above. The $S^*_{34}(\theta)$ signal can be zero at various θ even if no coefficients are zero. Among other matrix elements the S^*_{34} is highly structured and thus can be an excellent probe of scatterers.

ORD and CD Effects and the Scattering Matrix. ORD and CD are defined as the effects of the interaction of specific polarization states with a continuous slab of matter of well defined index of refraction. Both are strictly zero angle ($\theta = 0°$) effects, and no scattering is assumed. For particulate substances one can still define an operational index of refraction and make ORD and CD measurements (13). However, these data must be corrected for scattering effects which can become substantial as the particle size increases (5). The ORD and CD signals do not correspond to a particular matrix element; they are contained in the matrix as a whole. ORD and CD signals do not contain size, shape, and internal structure information about the scatterers which is contained in the scattering matrix.

THE EXPERIMENTAL SYSTEM

The experimental apparatus is described in detail in ref. 1 and is shown in Fig. 1. Monochromatic light with wavelength $\lambda_0 = 4420$ Å from a Cd-He laser is directed through a linear polarizer [P_1] and then through a photoelastic birefringence modulator [M] to modulate the polarization state of the incident beam. The incident light entering the scatterer can be completely characterized by the Stokes vector $|V_3|$

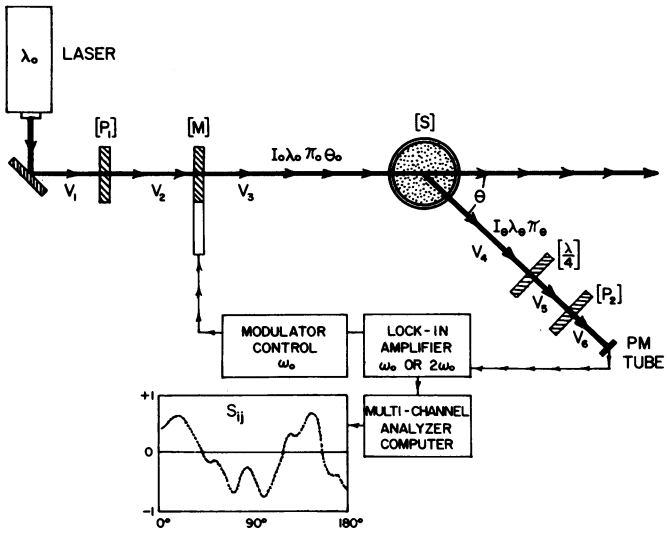

FIG. 1. The experimental scattering systems. Light from the laser is directed through the linear polarizer $[P_1]$ and birefringent modulator $[M]$, emerging in a state with intensity I_o, wavelength λ_o, polarization Π_o, and direction θ_o. It passes through the scatterers $[S]$, emerges at angle θ, and passes through the quarter wave plate $[\lambda/4]$ and linear polarizer $[P_2]$. Its intensity is detected by the photomultiplier tube. The detection frequency ω is selected by the lock-in amplifier. The resulting signal is digitized, stored in the computer, and printed out.

$= (I_3Q_3U_3V_3)$. The system of particles in the container scattering the incident light through angle θ is described mathematically by a scattering matrix $[S]$.

The outgoing light elastically scattered from the small particles can also be represented by a Stokes vector $|V_4|$ whose elements contain information about the scattering matrix elements. The scattered light, represented by Stokes vector $|V_6|$, is detected by a photomultiplier (EMI 9781B) in a telescope arm which is rotated from 0° to 168° by a stepping motor. Monochromatic filters, a quarter wave plate $[\lambda/4]$, and polarizer $[P_2]$ may be placed in front of the detector. The ac component of the photomultiplier signal is detected by a lock-in amplifier tuned to either the fundamental frequency (ω = 50 kHz), which is the natural frequency of the modulator, or the first harmonic frequency (ω = 100 kHz). For our experiments with biological samples, the output of the lock-in was fed to a computer. All signals were normalized by the total intensity. The θ-rotation of the telescope was synchronized to the dwell time per channel of the computer. Successive scans were stored in the computer memory. The final signal was printed out digitally by a Franklin printer.

To illustrate the mathematical technique for a specific case, refer to Fig. 1 and choose the following set of optical conditions: Set $[P_1]$ so its axis is at 45° to the scattering plane. Adjust $[M]$ so it is parallel to the scattering plane. Put $[S]$ in the light path, set $[P_2]$ so its axis is at 45° to the scattering plane. Remove the $[\lambda/4]$ plate. Unpolarized light $|V_1|$ passes through the optical elements and scattering cell and emerges in a final state given by Stokes vector $|V_5|$. The vector formed after passing through each optical component is calculated by multiplying the incident Stokes vector by the optical component matrix (14). Therefore $|V_2| = [P_1]\|V_1|$, $|V_3| = [M]\|V_2|$, $|V_4| = |V_5| = [S]\|V_3|$, and $|V_6| = [P_2]\|V_5| = [P_2][S][M][P_1]\|V_1|$. Following the procedure described in ref. 1, we get for the signal detected by the photomultiplier

$$I = \frac{C_1}{4}\left[1 + \left(\frac{S_{13} + S_{33}}{S_{11} + S_{31}}\right)C_2 \cos 2\omega t - \left(\frac{S_{14} + S_{34}}{S_{11} + S_{31}}\right)C_3 \sin \omega t\right]$$

where C_1, C_2, and C_3 are constants. When the lock-in is tuned to ω_o, , the amplified signal will be proportional to $(S_{14} + S_{34})/(S_{11} + S_{31}) \equiv S^*_{34}$. When tuned to $2\omega_o$, the signal is proportional to $(S_{13} + S_{33})/(S_{11} + S_{31})$. We can calibrate the signals by introducing *pure* polarization states into the detector, and adjusting the electronics to record full scale deflection (100%) for this pure state. By selecting various configurations of the polarizers $[P]$, modulator $[M]$, quarter wave plate $[\lambda/4]$, and lock-in frequency ω, other matrix elements and combinations can be printed out. The entire matrix $[S]$ can therefore be generated giving the total information accessible to elastic light scattering techniques.

Sample Selection and Preparation. In this study the spores of two strains of *Bacillus subtilis* were used to illustrate this technique. One of these strains, Marburg 168 (thy$^-$try$_2^-$), originally isolated by Farmer and Rothman (15), had normal spore structure. The other *Bacillus subtilis* strain UVS-42DPA has spores that lack dipicolinic acid (16), thus providing us a suitable structural modification. Both spore samples were prepared in the liquid Schaeffer medium (17) and cleaned by methods described by Tanooka *et al.* (18). Signals were obtained from spores in distilled water diluted to give single particle scattering.

RESULTS

Figs. 2–5 show the results. Fig. 2 shows the differential scattered light intensity S_{11} for both strains of spores. Although the curves are not normalized to equal numbers of scatterers, the phase of the signal structure is sufficiently different to permit the two kinds of spores to be distinguished. The polydispersion in size and shape of the spores destroys the signal structure on both curves at angles larger than about 70°.

Figs. 3A, 4A, and 5A show the additional information obtained from the S^*_{34}, $(S_{13} + S_{33})/(S_{11} + S_{31})$, and S_{12}/S_{11} signals, respectively, for the same spores. Each matrix element combination is plotted with the intensity scale in percent of full scale deflection. The maximum deflection for S^*_{34} (Fig. 3A) is about ±5% of full scale; for $(S_{13} + S_{33})/(S_{11} + S_{31})$ (Fig. 4A) it is about ±90%; for S_{12}/S_{11} (Fig. 5A) it is about +60%. Therefore, the $(S_{13} + S_{33})/(S_{11} + S_{31})$ is the largest signal, the S^*_{34} the smallest.

All three curves have structure. Structure occurs when the slope changes either sign or magnitude. The largest structure occurs on S^*_{34}, where its magnitude is about 25% of the total signal strength. The smallest structure occurs on $(S_{13} + S_{33})/(S_{11} + S_{31})$, where its magnitude is only about 10% of the total signal strength. The large structure on S^*_{34} makes it a visually dramatic signal.

Specific theoretical interpretation of the scattering signal is not possible at this time. For the curves to be useful, we must rely on the ability of two different scatterers to give two different curves. *Visually* without further analysis, the S^*_{34} curve shows differences that are more dramatic than those of $(S_{13} + S_{33})/(S_{11} + S_{31})$ or the S_{12}/S_{11}. This is true for a variety of biological systems we studied: guinea pig red blood cells, guinea pig lymphocytes, human red blood cells, human lymphocytes, ribosomes, one globular protein, vari-

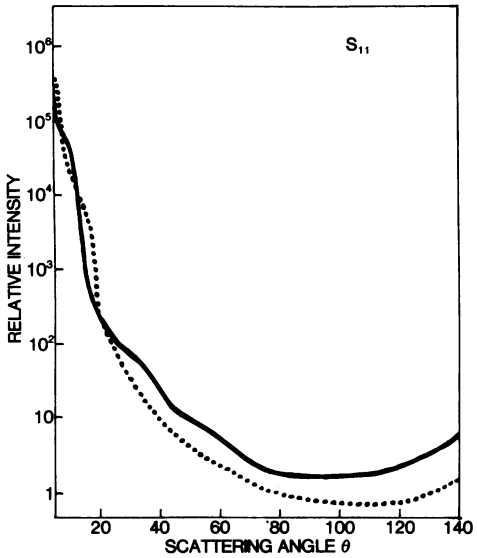

FIG. 2. Differential scattered light intensity signals S_{11} for spores of Marburg 168 (····) and UVS-42DPA (—) strains. The curves are not normalized to equal number of scatterers.

ous buffer solutions, temperature-time dependent development, and two mutant varieties of bacterial spores, which we report in detail here. In all cases, the S^*_{34} signal survived as a *unique indicator* of that scatterer.

The most important point is that significant structure appears on the other $S_{ij}(\theta)$ signals even if it is weak or absent in the S_{11} matrix element, which is the differential scattered light intensity signal. All of our signals are averaged over all possible orientations of many scatterers. Our work, and that of others (19) who examined only S_{11}, show clearly that biological systems have unique scattering matrices in spite of the average over particle orientation. The integral over all particle orientations fortunately contributes only small deviations to the scattering matrix element which characterize the system.

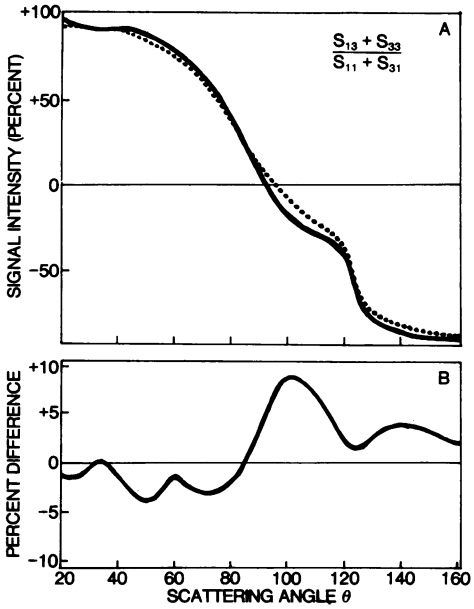

FIG. 4. (A) The $(S_{13} + S_{33})/(S_{11} + S_{31})$ signals as a function of scattering angle for spores of Marburg 168 (····) and UVS-42DPA (—). (B) Percent differences between the two signals.

Figs. 3B, 4B, and 5B show the percent differences in the respective signals from each set of spores. The difference curves are measures of the correlation or similarity of the signals. Since all the difference curves are non-zero *and* highly structured, any one of the three can be a probe to characterize the scatterer. The point is clear, however, that several or all matrix element signals together become an extremely powerful method for distinguishing between biological entities that may differ only slightly from each other.

We have also analyzed the S^*_{34} signal by taking its Fourier transform. Our preliminary results give three frequency components for the spores of Marburg 168 strain and only two for the UVS-42DPA strain. The application of differ-

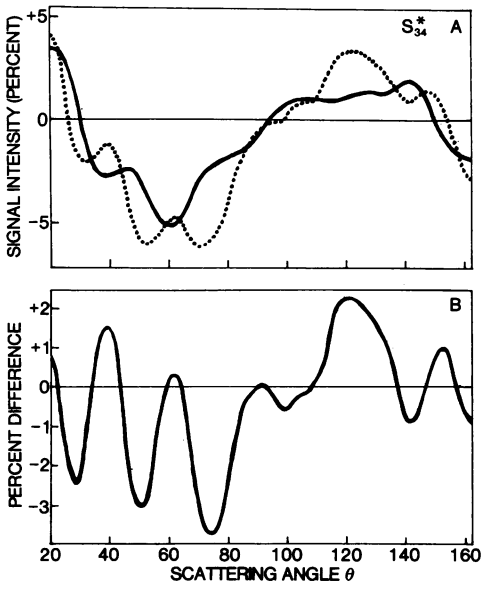

FIG. 3. (A) The S^*_{34} signals as a function of scattering angle for spores of Marburg 168 (····) and UVS-42DPA (—). (B) Percent differences between the two S^*_{34} signals.

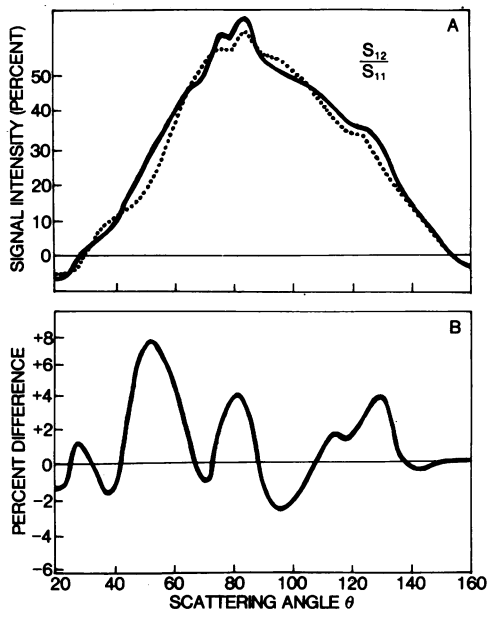

FIG 5. (A) The S_{12}/S_{11} signals as a function of scattering angle for spores of Marburg 168 (·····) and UVS-42DPA (—). (B) Percent differences between the two signals.

ence curves and Fourier transforms to the scattering curves will give an unbiased computer analysis of their features and permit correlations to be done for "similar systems" or for time dependent events.

CONCLUSIONS AND DISCUSSION

This study has shown that the polarization effects in light scattering are useful as a major tool in biological research. We have shown that certain elements of the scattering matrix and some of their combinations are especially sensitive to minute structural modifications of the scatterer. We have also shown that some of the information that may be lost or barely detectable in the differential scattered light intensity (S_{11}) profoundly changes the scattering signals of other matrix elements and combinations, especially in the S^*_{34}. This combination is measured directly with our present instrument. It has given a unique and characteristic signal for every scattering particle of biological origin that we have surveyed in our preliminary studies. Detailed experimental results of *B. subtilis* spores have been reported in this publication. One of these spores, UVS-42DPA, is a structurally modified strain lacking in dipicolinic acid. Thus, the scattering signal modification corresponds to this modification in the spore structure.

Despite the theoretical difficulties of calculating the structure or structural modification of the scatterer directly from the scattering data, this technique has powerful applications in cell and molecular biology. Our preliminary survey work shows it is a sensitive indicator of structural changes in time dependent phenomena of life cycles of cells. By studying model systems of known structures where we can introduce known structural modifications it should be possible to develop at least a semi-empirical understanding of the physical meaning of some of the more complex matrix elements and their combinations such as S^*_{34}.

Due to the high characteristic specificity of the scattering signals this technique has great potential for applications to microbial typing and taxonomy, in studies of cell structure, time dependent studies of cell regulation, cell differentiation, cell transformation, and drug effects. In the visible wavelength region the method is nondestructive and can be used to monitor cellular activities over long time periods.

The studies presented here have been performed on suspensions of many scatterers; however, they can be readily extended to scattering from a single particle using methods similar to Wyatt and Phillips (2), or to *resonance* scattering to monitor structural changes in scatterers (7, 20, 21).

Another natural application of this technique is in the ultraviolet wavelength region (λ 2000–3000 Å). Work by Maestre and Tinoco (3, 4) has shown very strong ORD and CD signals in the ultraviolet. Their work on viruses has shown that ORD and CD signals are unique for each virus type and are determined primarily by the virus nucleic acid binding state and packing. The signals are very sensitive to even the slightest modification in the virus nucleoprotein arrangement. Subsequent studies (5, 6) have shown that polarization effects due to Mie scattering contribute substantially to the ORD and CD signals. Bohren (12, 13) has made theoretical calculations of the Mie scattering of optically active substances. Thus, the extension of the study of the complete scattering matrix into the ultraviolet range should give us a new sensitive tool for studying nucleoproteins, especially for the study of events occurring in the cell nucleus where other techniques are difficult to apply and the present knowledge is yet lacking. These studies should give us information about the binding states and packing of the cellular DNA as well as give useful information about the time sequence of conformational changes in the cell nucleus to be correlated with other biological and biochemical observations.

We thank Drs. W. S. Jeter and W. S. Cozine for providing us with a variety of biological specimens for our survey studies; Dr. H. Tanooka for providing us with bacterial spores; Dr. H. C. van de Hulst for his comments on scattering theory; and Dr. A. J. Hunt for valuable discussions.

1. Hunt, A. J. & Huffman, D. R. (1973) *Rev. Sci. Instrum.* **44**, 1753–1762.
2. Wyatt, P. J. & Phillips, D. T. (1972) *J. Theor. Biol.* **37**, 493–501.
3. Maestre, M. F. & Tinoco, I. (1965) *J. Mol. Biol.* **12**, 287–289.
4. Maestre, M. F. & Tinoco, I. (1967) *J. Mol. Biol.* **23**, 323–335.
5. Holzwarth, G., Gordon, D. G., McGinness, J. E., Dorman, B. P. & Maestre, M. F. (1974) *Biochemistry* **13**, 126–132.
6. Gordon, D. J. & Holzwarth, G. (1971) *Proc. Nat. Acad. Sci. USA* **68**, 2365–2369.
7. van de Hulst, H. C. (1957) *Light Scattering by Small Particles* (Wiley, New York).
8. Hunt, A. J. (1974) Ph.D. Dissertation, University of Arizona.
9. Mie, G. (1908) *Ann. Phys. (Leipzig)* **25**, 377–445.
10. Lind, A. C. & Greenburg, J. M. (1966) *J. Appl. Phys.* **37**, 3195–3203.
11. Ruppin, R. & Engleman, R. (1970) *Rep. Prog. Phys.* **33**, 149–196.
12. Bohren, C. F. (1974) *Chem. Phys. Lett.* **29**, 458–462.
13. Bohren, C. F. (1975) *J. Chem. Phys.* **62**, 1566–1571.
14. Shurcliff, W. A. (1966) *Polarized Light* (Harvard University Press, Cambridge).
15. Farmer, J. L. & Rothman, F. (1965) *J. Bacteriol.* **89**, 262–263.
16. Zytkovicz, T. H. & Halvorson, H. O. (1972) in *Spores. V.*, eds. Halvorson, H. O., Hanson, R. & Campbell, L. L. (American Society for Microbiology, Washington, D.C.), pp. 49–52.
17. Takahashi, I. (1965) *J. Bacteriol.* **89**, 294–298.
18. Tanooka, H., Terano, H. & Otsuka, H. (1971) *Biochim. Biophys. Acta* **228**, 26–37.
19. Salzman, G. C., Crowell, J. M., Goad, C. A., Hansen, K. M., Hiebert, R. D., LaBauve, P. M., Martin, J. C., Ingram, M. L. & Mullaney, P. F. (1975) *Clin. Chem.* **21**, 1297–1304.
20. Kerker, M. (1969) *The Scattering of Light and Other Electromagnetic Radiation* (Academic Press, New York).
21. Marshall, T. R., Parmenter, C. S. & Seaver, M. (1975) *Science* **190**, 375–377.